Journal of Medical Microbiology and Infectious Diseases

JoMMID
ISSN: 2345-5349
eISSN: 2345-5330

Temporal Changes in Long Non-Coding RNA HULC Expression in Hepatitis B Virus-Associated Hepatocellular Carcinoma Cells Infected with Oncolytic Reovirus: An *In Vitro* Study

Reihaneh Kazemi[1], Mojtaba Hamidi-Fard[2]*, Elham Siasi[3], Mohammad Reza Aghasadeghi[2], Pooneh Rahimi[2]

[1]Department of Genetics, NT.C., Islamic Azad University, Tehran, Iran; [2]Department of Hepatitis and AIDS, Pasteur Institute of Iran, Tehran, Iran; [3]Department of Microbiology, NT.C., Islamic Azad University, Tehran, Iran

ARTICLE INFO

Original Article

Keywords: Hepatocellular carcinoma, Hepatitis B virus, HULC, Long non-coding RNA, Mammalian orthoreovirus, Oncolytic virotherapy

Received: 06 Jun. 2026
Received in revised form: 24 Aug. 2026
Accepted: 12 Oct. 2026
DOI: [To be assigned]

***Correspondence**
Email: mojtaba_hamidifard@yahoo.com

© The Author(s)

ABSTRACT

Introduction: HULC is a long non-coding RNA (lncRNA) implicated in hepatocellular carcinoma (HCC), including hepatitis B virus (HBV)-associated disease. Mammalian orthoreovirus (reovirus) exhibits oncolytic activity in experimental cancer models. This study examined temporal changes in HULC expression and intracellular reovirus RNA in patient-derived HBV-associated HCC cells and Huh-7 cells following infection. **Methods:** Both cell models were exposed to reovirus at a multiplicity of infection of 10. Cells were collected at 0, 24, 48, and 72 hours post-infection (hpi). HULC expression and reovirus L1 RNA were assessed by reverse-transcription quantitative PCR (RT-qPCR); cell metabolic activity and viability were examined using MTT and trypan blue assays, respectively. **Results:** Reovirus L1 threshold-cycle values decreased over time in both cell models, consistent with increasing intracellular viral RNA abundance, with the lowest values at 72 hpi. Relative HULC expression increased at 24 and 48 hpi and decreased below the 0-hpi reference at 72 hpi. At 24 and 48 hpi, HULC fold changes were greater in the patient-derived cells than in Huh-7 cells; this relationship was reversed at 72 hpi. Both cell types showed reduced metabolic activity and viability during infection. **Conclusion:** Reovirus exposure was associated with a transient increase in HULC expression followed by reduced expression at 72 hpi. These descriptive findings do not establish that HULC regulates viral replication or that the effect is HBV-specific. Confirmation using additional biological replicates, time-matched uninfected controls, and infectious-virus assays is required.

INTRODUCTION

Hepatocellular carcinoma (HCC) is the most prevalent primary liver malignancy and is among the leading causes of cancer-related death worldwide [1]. Chronic hepatitis B virus (HBV) infection is an important etiological factor, particularly in regions where HBV infection is endemic [2].

The mechanisms underlying HBV-associated hepatocarcinogenesis include viral DNA integration into the host genome, expression of viral proteins such as HBx, and dysregulation of regulatory RNAs, including microRNAs and long non-coding RNAs (lncRNAs) [3].

Among lncRNAs implicated in HCC, HULC (highly upregulated in liver cancer), located on chromosome 6p24.3, is an extensively studied transcript reported to be overexpressed in HCC tissue [4]. Experimental studies have implicated HULC in cell-survival signaling, autophagy, invasion, and metabolic reprogramming [5, 6]. HULC has also been investigated in HBV-associated HCC, although its expression and regulatory effects may depend on the biological context [7].

Treatment options for HCC include resection, transplantation, locoregional therapies, systemic targeted agents, and immunotherapy; recurrence, treatment resistance, and disease stage remain important challenges [8, 9]. Oncolytic virotherapy is under investigation because certain viruses can damage tumor cells and stimulate antitumor immunity [10]. Mammalian orthoreovirus (reovirus), a non-enveloped virus with a segmented double-stranded RNA genome in the family *Spinareoviridae*, can show enhanced oncolytic activity in susceptible tumor cells; activated Ras signaling is one of several factors implicated in this susceptibility [11, 12]. Previous studies have described reovirus-induced cytotoxicity in experimental HCC models [13, 14].

[Downloaded from jommid.pasteur.ac.ir on 2026-11-16]

However, temporal changes in HULC expression following reovirus exposure in HCC cells have not been well characterized. We therefore examined intracellular reovirus L1 RNA abundance, HULC expression, metabolic activity, and cell viability in patient-derived HBV-associated HCC cells and Huh-7 cells at several post-infection time points. This comparison was exploratory and was not designed to establish a specific causal effect of HBV on reovirus susceptibility.

MATERIAL AND METHODS

Establishment of patient-derived HBV-associated HCC cultures. Cultures were established from material obtained by ultrasound-guided fine-needle aspiration (FNA) from a patient with confirmed HBV-associated HCC, according to a previously described approach [14]. The specimen was transported to the Pasteur Institute of Iran under sterile, temperature-controlled conditions. Mechanical processing was followed by explant culture, from which adherent cells were isolated by outgrowth. Experiments were performed with passage 3 cells.

Cell culture and maintenance. Huh-7 cells and patient-derived HBV-associated HCC cultures were maintained in 75-cm² flasks containing Dulbecco's modified Eagle medium (DMEM; Gibco, Thermo Fisher Scientific, USA) supplemented with 10% fetal bovine serum (Gibco) and 1% penicillin–streptomycin (stock concentration, 10,000 U/mL; Gibco). Cultures were incubated at 37°C in a humidified atmosphere containing 5% CO_2. At approximately 70-80% confluence, cells were detached using 0.25% trypsin–EDTA (Gibco), collected, and reseeded for subsequent experiments.

Reovirus propagation. Mammalian orthoreovirus type 3 Dearing (T3D) was propagated in L929 cells. Monolayers were washed twice with phosphate-buffered saline (PBS; Gibco, Thermo Fisher Scientific, USA) and exposed to reovirus at 37°C for 90 min. Serum-free medium was then added, and cultures were maintained until cytopathic effects (CPEs) were evident in more than 80% of cells. The cultures underwent three freeze–thaw cycles; clarified supernatants were collected as working viral stocks. The infectious titer and methods used to determine the stated multiplicity of infection were not reported.

Assessment of reovirus-associated cytotoxicity using the MTT assay. Patient-derived HBV-associated HCC cells and Huh-7 cells were seeded in separate wells of 96-well plates at 1×10^4 cells per well. After 24 h, cultures were exposed to reovirus at a reported multiplicity of infection (MOI) of 10 and evaluated at 0, 24, 48, and 72 hpi. Three technical replicate wells were used per time point. Uninfected cells and medium-only wells served as control and blank wells, respectively. At each time point, medium was removed and replaced with 100 µL of RPMI-1640 (Gibco), followed by 10 µL of 12 mM MTT solution (Sigma-Aldrich, USA). Following incubation for 4 h, 50 µL of dimethyl sulfoxide (Sigma-Aldrich, USA) was added to solubilize the formazan. Plates were mixed, incubated at 37°C for 10 min, and read at 570 nm using an Epoch 2 microplate spectrophotometer (BioTek, USA). MTT absorbance was interpreted as a measure of metabolic activity rather than a direct cell count.

Reovirus infection and time-point sampling. Huh-7 and patient-derived HBV-associated HCC cells were seeded in separate six-well plates and infected with reovirus at a reported MOI of 10. Cells were sampled at 0, 24, 48, and 72 hpi. A single uninfected well was included in each experimental set; however, separate time-matched uninfected controls were not available for each post-infection interval. Accordingly, the 0-hpi comparator does not isolate infection effects from time-dependent changes associated with continued culture. Samples were processed for RNA extraction or stored at -80°C.

Cell viability assessment in reovirus-exposed cells. Cell viability was assessed at 0, 24, 48, and 72 hpi by trypan blue exclusion (Gibco, Thermo Fisher Scientific, USA). Viability was determined using the following equation:

Cell viability (%) = (number of viable cells / total number of counted cells) × 100.

Experiments were performed in duplicate.

RNA extraction and cDNA synthesis. Total RNA was isolated from harvested cell pellets using the FavorPrep Tissue Total RNA Mini Kit (Favorgen Biotech, Taiwan), following the manufacturer's instructions. RNA concentration and purity were assessed using a NanoDrop spectrophotometer (Thermo Fisher Scientific, USA). The reported A_{260}/A_{280} ratios ranged from 1.8 to 2.0. cDNA was prepared using the RevertAid First Strand cDNA Synthesis Kit (Thermo Fisher Scientific, USA) and stored at -20°C.

Assessment of reovirus L1 RNA by RT-qPCR. Intracellular reovirus RNA was assessed using SYBR Green-based RT-qPCR targeting the L1 genome segment. Each 20 µL reaction contained 10 µL of 2× qPCRBIO SyGreen Mix (PCR Biosystems, UK), 0.4 µL of each primer (Table 1), 2 µL of cDNA, and 7.2 µL of nuclease-free water. The TATA-binding protein (TBP) target was also amplified as a cellular control. Assays were performed in technical duplicate with a negative control. Cycling conditions were 95°C for 3 min, followed by 40 cycles of 95°C for 15 s, 58°C for 30 s, and 72°C for 30 s. Melting curves were examined for a dominant amplification product. Viral RNA was reported as raw threshold-cycle (Ct) values rather than as an absolute quantity or infectious titer.

[Downloaded from jommid.pasteur.ac.ir on 2026-11-16]

Quantification of HULC expression by RT-qPCR. HULC RNA levels were determined using PowerUp SYBR Green Master Mix (Applied Biosystems, USA) on a StepOnePlus real-time PCR system (Applied Biosystems, USA). Each 20 µL reaction contained 10 µL of 2× master mix, 0.5 µL of each primer (Table 1), 2 µL of cDNA, and 7 µL of nuclease-free water. A no-template control was included. TBP was selected as the reference gene on the basis of previously published studies in HCC [15, 16]; its stability across the present infection conditions was not independently demonstrated. Cycling conditions were 95°C for 10 min followed by 40 cycles of 95°C for 15 s, 60°C for 30 s, and 72°C for 30 s. Melting curve analysis was conducted to assess amplification specificity.

Relative HULC expression was calculated using the $2^{-\Delta\Delta Ct}$ method, with 0-hpi samples as the calibrator. Measurements at 24, 48, and 72 hpi were expressed relative to that reference. Two independent biological replicates were reported, each analyzed in technical duplicate.

Table 1. Primer sequences used for RT-qPCR analysis of the reovirus L1 segment and human HULC and TBP targets.

Target Gene	Primer Type	Sequence (5′–3′)	Reference
L1	Forward	CATATGACTACCACTTTCCCG	[17]
	Reverse	GCTATGTCATATTTCCATCCG	
TBP	Forward	TGCACAGGAGCCAAGAGTGAA	[18]
	Reverse	CACATCACAGCTCCCCACCA	
HULC	Forward	ATCTGCAAGCCAGGAAGAGTC	[19]
	Reverse	CTTGCTTGATGCTTTGGTCTGT	

Note: TBP was used as the endogenous reference for HULC normalization. Published references do not substitute for experimental validation of primer specificity and amplification efficiency under the conditions used.

Statistical analysis. Data are presented as means ± standard deviations (SDs). Reovirus L1 results are summarized as cycle threshold (Ct) values, with lower values generally indicating greater template abundance when amplification efficiency is comparable. Relative HULC expression was calculated as $\Delta Ct = Ct(HULC) - Ct(TBP)$ and $\Delta\Delta Ct = \Delta Ct(\text{time point}) - \Delta Ct(0\ \text{hpi})$. Because the experiments were limited to two independent biological replicates, robust statistical significance could not be established; therefore, no significance testing was conducted for the RT-qPCR data, and although nominal *P*-value thresholds are displayed in Figures 2 and 3, all comparisons throughout the manuscript are interpreted descriptively.

RESULTS

Cell culture and morphology. Both cell models were cultured in DMEM supplemented with 10% fetal bovine serum and 1% penicillin–streptomycin at 37°C in 5% CO_2. At 48 h, the cultures were approximately 80–90% confluent and showed adherent cellular morphology on light microscopy (Figure 1). Morphology alone did not establish the identity or purity of the patient-derived cultures.

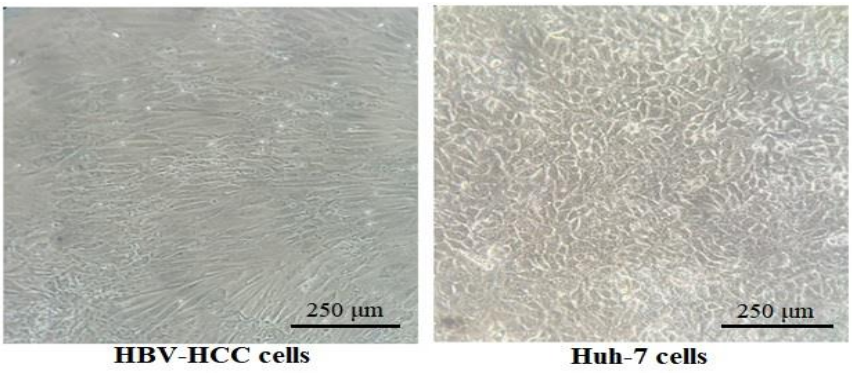


Fig. 1. Representative light-microscopic images of patient-derived HBV-associated HCC cultures and Huh-7 cells after 48 h in culture (original magnification, ×10; scale bars, 250 µm).

Assessment of reovirus-associated cytotoxicity by MTT assay. MTT absorbance declined over time in both cell models following reovirus exposure (Figure 2). The patient-derived cells showed lower absorbance than Huh-7 cells at 24, 48, and 72 hpi, consistent with lower metabolic activity under the conditions studied. These measurements do not, by themselves, distinguish cell death from reduced metabolic activity or proliferation.

[Downloaded from jommid.pasteur.ac.ir on 2026-11-16]

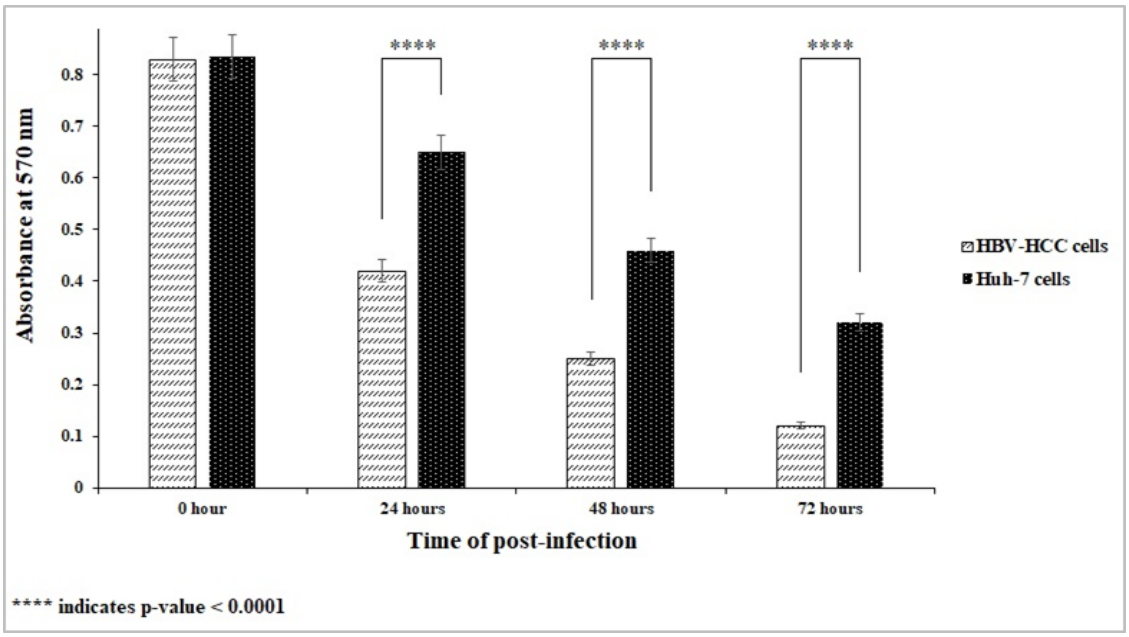


Fig. 2. MTT assay of patient-derived HBV-associated HCC cells and Huh-7 cells after reovirus exposure (MOI = 10). Absorbance at 570 nm declined at 24, 48, and 72 hpi. The patient-derived cultures had lower absorbance than Huh-7 cells at the post-infection time points (24–72 hpi).

Cell viability following reovirus exposure. Cell rounding and clumping were observed beginning at approximately 24 hpi. Trypan blue exclusion showed a decline in viable-cell percentages in both cell models between 0 and 72 hpi (Figure 3). Viability was lower in the patient-derived HBV-associated HCC cells than in Huh-7 cells at 24, 48, and 72 hpi, as shown in the figure.

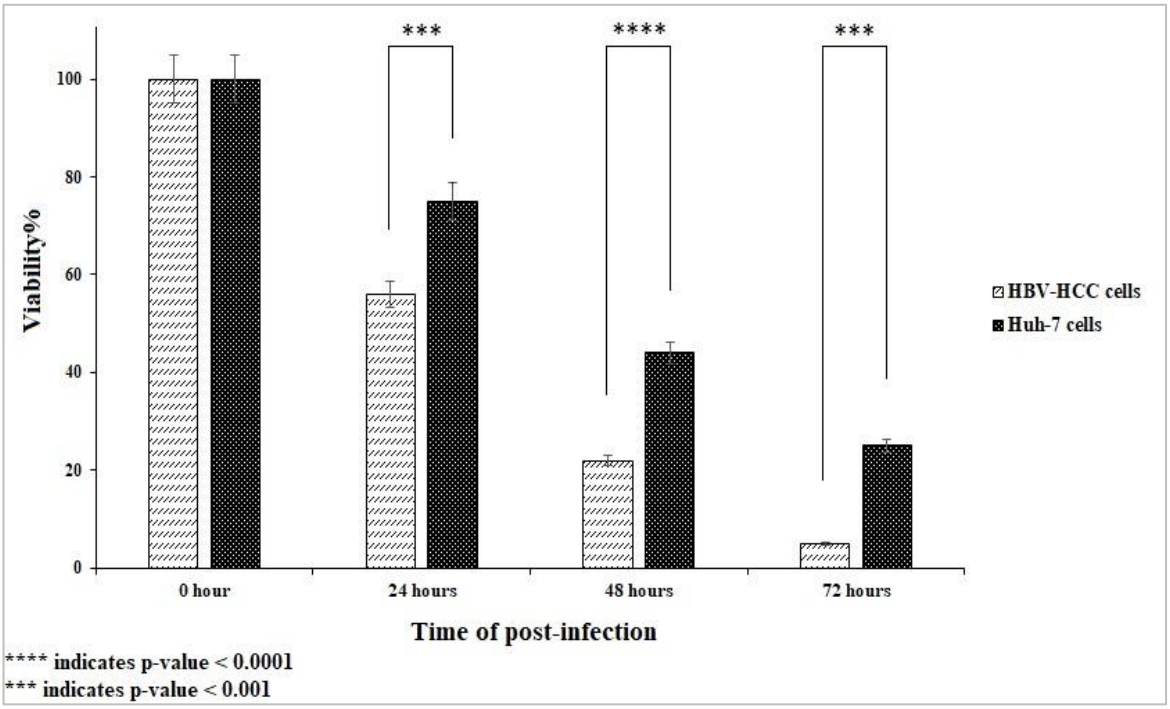


Fig. 3. Trypan blue viability measurements in patient-derived HBV-associated HCC cells and Huh-7 cells after reovirus exposure (MOI = 10). Viability declined over 72 h in both models and was lower in the patient-derived cultures at 24, 48, and 72 hpi.

[Downloaded from jommid.pasteur.ac.ir on 2026-11-16]

Assessment of intracellular reovirus RNA by RT-qPCR. The reported L1 Ct values declined over time in both cell models, consistent with increasing detectable intracellular reovirus RNA.

At 0 hpi, mean L1 Ct values were 24.15 ± 0.21 in Huh-7 cells and 21.20 ± 0.14 in patient-derived HBV-associated HCC cells, indicating different initial detectable viral RNA levels. At 24 hpi, the corresponding values were 19.80 ± 0.28 and 17.50 ± 0.14; at 48 hpi, 18.38 ± 0.02 and 16.70 ± 0.14; and at 72 hpi, 17.95 ± 0.07 and 16.36 ± 0.04. These results indicate a time-dependent decrease in Ct values in both cell models. However, the baseline difference and absence of a normalized viral RNA measure preclude a definitive comparison of replication rates between cell models.

As shown in Figure 4, patient-derived cultures had lower L1 Ct values than Huh-7 cells at each time point, including baseline. Melting curve peaks near 83°C for L1 and 84°C for TBP were reported. A single melting peak is consistent with a dominant amplification product but does not, alone, verify target identity, RT efficiency, or infectious-virus production.

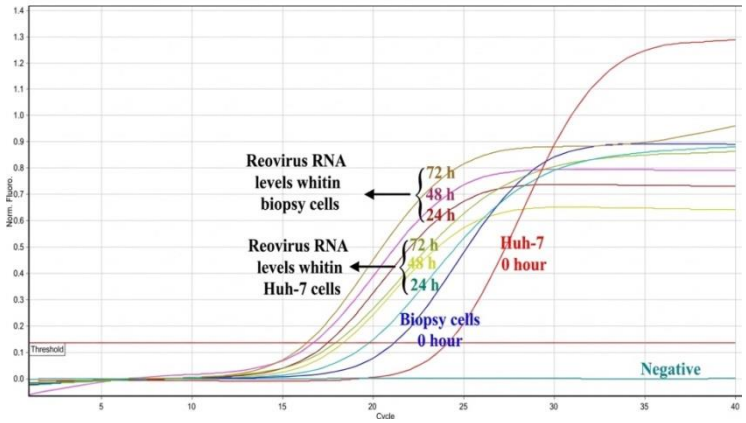


Fig. 4. Representative RT-qPCR amplification curves for the reovirus L1 target in patient-derived HBV-associated HCC cells (labeled as biopsy cells) and Huh-7 cells at 0, 24, 48, and 72 hpi. Lower Ct values suggest greater detectable L1 RNA under comparable assay conditions.

Quantification of HULC expression by RT-qPCR. HULC expression was assessed in both cell models at 0, 24, 48, and 72 hpi. Ct values for HULC were normalized to TBP, and relative expression was calculated using the 0 hpi sample as the reference.

The reported HULC and TBP amplification curves changed across sampling times (Figures 5 and 6). However, a visual shift in unnormalized amplification curves cannot alone establish upregulation or downregulation of HULC. Interpretation requires the corresponding ΔCt and ΔΔCt calculations provided in Tables 2 and 3.

By 72 hpi, both cell models showed markedly reduced viability. Changes in cellular composition, RNA integrity, and reference-gene stability may therefore influence apparent relative HULC expression at this late time point. The study did not measure whether these factors accounted for the observed decrease.

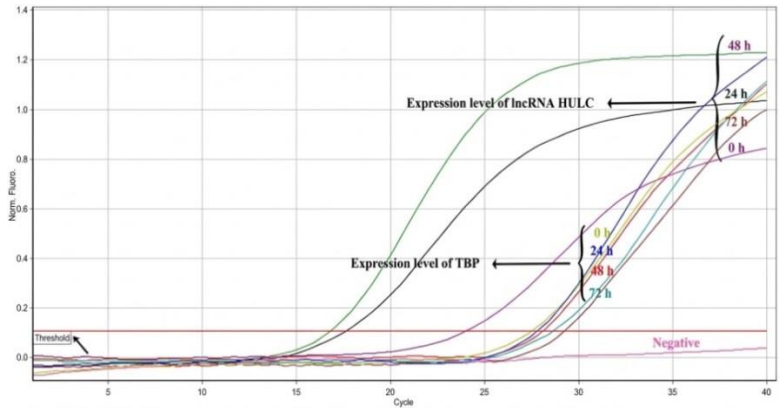


Fig. 5. Representative RT-qPCR amplification curves for HULC and TBP in Huh-7 cells at 0, 24, 48, and 72 hpi. Relative expression estimates were calculated separately from the Ct values using the $2^{-\Delta\Delta Ct}$ method (Table 2).

[Downloaded from jommid.pasteur.ac.ir on 2026-11-16]

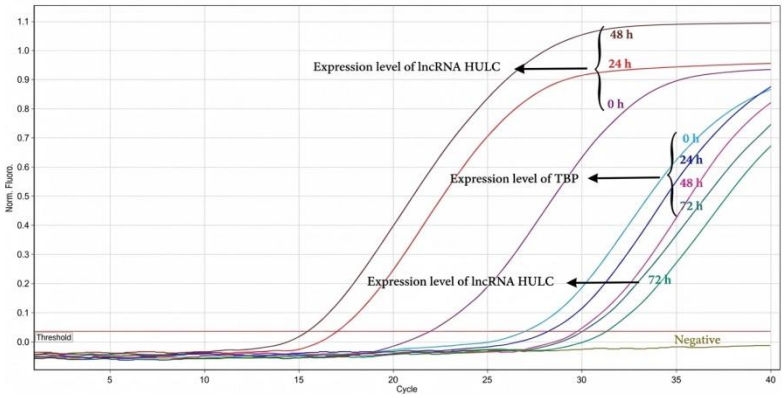


Fig. 6. Representative RT-qPCR amplification curves for HULC and TBP in patient-derived HBV-associated HCC cells at 0, 24, 48, and 72 hpi. Relative expression estimates were calculated separately from the Ct values using the $2^{-\Delta\Delta Ct}$ method (Table 3).

In Huh-7 cells (Table 2), mean HULC fold changes relative to 0 hpi were 102.40 ± 3.39 at 24 hpi, 198.70 ± 5.23 at 48 hpi, and 0.21 ± 0.03 at 72 hpi. Thus, the reported relative expression peaked at 48 hpi and was below the baseline reference at 72 hpi.

Table 2. Reported HULC RT-qPCR measurements in Huh-7 cells (0-72 hpi).

Sample (hpi)	Ct HULC (Mean ± SD)	Ct TBP (Mean ± SD)	ΔCt (Mean ± SD)	ΔΔCt (Mean ± SD)	Relative expression ($2^{-\Delta\Delta Ct}$) (Mean ± SD)
0	24.00 ± 0.10	27.50 ± 0.10	-3.50 ± 0.14	0.00 ± 0.00	1.00 ± 0.00
24	17.62 ± 0.05	27.80 ± 0.10	-10.18 ± 0.11	-6.68 ± 0.11	102.40 ± 3.39
48	16.87 ± 0.08	28.00 ± 0.12	-11.13 ± 0.14	-7.63 ± 0.14	198.70 ± 5.23
72	27.75 ± 0.10	29.00 ± 0.15	-1.25 ± 0.18	2.25 ± 0.18	0.21 ± 0.03

Patient-derived HBV-associated HCC cells showed the same direction of temporal change (Table 3): reported mean HULC fold changes were 148.90 ± 5.52 at 24 hpi, 305.20 ± 3.96 at 48 hpi, and 0.051 ± 0.004 at 72 hpi. These estimates are descriptive and require confirmation with more biological replicates.

Table 3. Reported HULC RT-qPCR measurements in patient-derived HBV-associated HCC cells (0-72 hpi).

Sample (hpi)	Ct HULC (Mean ± SD)	Ct TBP (Mean ± SD)	ΔCt (Mean ± SD)	ΔΔCt (Mean ± SD)	Relative expression ($2^{-\Delta\Delta Ct}$) (Mean ± SD)
0	22.00 ± 0.10	27.50 ± 0.10	-5.50 ± 0.14	0.00 ± 0.00	1.00 ± 0.00
24	15.67 ± 0.08	28.40 ± 0.12	-12.73 ± 0.14	-7.23 ± 0.14	148.90 ± 5.52
48	16.05 ± 0.10	29.80 ± 0.15	-13.75 ± 0.18	-8.25 ± 0.18	305.20 ± 3.96
72	30.00 ± 0.12	31.20 ± 0.18	-1.20 ± 0.22	4.30 ± 0.22	0.051 ± 0.004

At 24 and 48 hpi, HULC fold changes were numerically higher in the patient-derived cultures than in Huh-7 cells, whereas at 72 hpi, the relative expression was lower in the patient-derived cells (0.051 versus 0.210).

DISCUSSION

We investigated temporal changes in intracellular reovirus L1 RNA and HULC expression after exposing patient-derived HBV-associated HCC cells and Huh-7 cells to reovirus. In both models, L1 Ct values decreased over time, whereas HULC fold changes increased at 24–48 hpi and declined below the 0-hpi reference at 72 hpi. The intracellular RNA findings are compatible with increasing detectable viral RNA, but they do not establish the quantity of infectious virus produced [20–25]. To our knowledge, this specific temporal pattern of HULC expression has not previously been described in these models; the present observational design does not identify its mechanism.

Early increases in HULC expression coincided with declining reovirus L1 Ct values. Previous studies have shown that HULC can participate in hepatitis C virus (HCV) infection and in HBV-associated replication pathways [26–28]. These findings concern distinct viruses and cannot be assumed to describe HULC function during reovirus infection. At 72 hpi, relative HULC expression was lower while intracellular L1 RNA remained readily detectable. This divergence could reflect infection-associated cellular stress, changing cell viability, or reference-gene instability; direct viral suppression of HULC was not tested. Host and viral lncRNAs have diverse roles in virus–host interactions [29], but this general literature does not establish a reovirus-specific suppression mechanism.

[Downloaded from jommid.pasteur.ac.ir on 2026-11-16]

The two cell models differed in MTT absorbance, trypan blue viability, and L1 Ct values. A prior study has demonstrated the antitumor and antiviral activity of oncolytic reovirus in liver cancer models [30]; however, that study does not establish that HBV positivity independently causes greater reovirus replication than HBV negativity. HBx and other HBV-associated factors can alter cellular signaling and non-coding RNA regulation [31–33]. Whether such changes contributed to the present findings remains unknown because the models also differed in patient origin, culture history, and potentially other properties, and no direct manipulation of HBV or HBx was performed.

Several limitations affect interpretation. Only one patient-derived culture and one established HCC cell line were examined. Biological replication for RT-qPCR was limited to two independent experiments. Separate, time-matched uninfected wells were not available for every collection time, and the L1 signal differed between models at baseline. Thus, later changes cannot be attributed exclusively to infection, nor can between-model differences be interpreted as HBV-specific effects. The analysis included no measured infectious-virus titers, no validation of reference-gene stability during infection, and no independent confirmation of viral RNA abundance normalized to cell number or input. In addition, no experiment manipulating HULC expression was performed, preventing causal inference.

Future studies should include authenticated and independently derived HCC models, standardized infectious input, time-matched mock-infected controls, a larger number of independent biological replicates, and plaque or equivalent infectivity assays. Confirmation of primer specificity and amplification efficiency, assessment of TBP stability during infection, and HULC knockdown or overexpression experiments would help distinguish biological regulation from late-stage cell-loss effects. Additional early sampling may clarify the onset of RNA changes.

In conclusion, reovirus exposure was associated with declining L1 Ct values, loss of metabolic activity and viability, and a biphasic pattern of relative HULC expression in two HCC-derived culture models. The findings are preliminary and do not demonstrate that HULC controls reovirus replication or that HBV association alone accounts for the observed differences. Mechanistic and independently replicated studies are needed before translational conclusions can be drawn.

ACKNOWLEDGMENT

The authors thank the staff of the Department of Hepatitis and AIDS, Pasteur Institute of Iran, for their support and the participant who consented to the research use of biopsy-derived material.

CONFLICTS OF INTEREST

The authors declare that there are no conflicts of interest associated with this manuscript.

FUNDING

This research was supported by a grant from the Pasteur Institute of Iran (Grant No. 2229).

AI DISCLOSURE

The authors reported no AI use in preparing the submitted manuscript.

DATA AVAILABILITY

The summary data supporting the findings of this study are presented in the manuscript. The underlying replicate-level data for the RT-qPCR, MTT (metabolic activity), and cell viability assays are available from the corresponding author upon reasonable request.

AUTHORS' CONTRIBUTIONS

RK was responsible for data collection, conducted the preliminary analysis, and drafted the initial version of the manuscript. MH-F led the conceptualization and design of the study, supervised the overall project, and performed the principal data analysis and interpretation. ES carried out the statistical analysis and contributed to editing the manuscript. MRA assisted with data interpretation and validation, and provided technical support. PR contributed to data interpretation and the literature review, and assisted with editing and formatting the manuscript for clarity and consistency. All authors have reviewed and approved the final manuscript and agree to be accountable for all aspects of the work.

ETHICS STATEMENT

Ethical approval for the collection and research use of human-derived material was reported from the Ethics Committee of the Pasteur Institute of Iran (No. IR.PII.REC.1402.035). The authors state that written informed consent was obtained for the collection and research use of the biopsy-derived specimen, including establishment of primary cultures, and that procedures followed the Declaration of Helsinki.

REFERENCES

1. Mauro E, de Castro T, Zeitlhoefler M, Sung MW, Villanueva A, Mazzaferro V, et al. Hepatocellular carcinoma: epidemiology, diagnosis and treatment. JHEP Rep. 2025;7(12):101571.
2. Méndez-Sánchez N, Valencia-Rodríguez A, Coronel-Castillo CE, Qi X. Narrative review of hepatocellular carcinoma: from molecular bases to therapeutic approach. Dig Med Res. 2021;4:15.
3. Ma L, Chen S, Wang H, Chen L. Hepatitis B virus integration and hepatocarcinogenesis. Liver Res. 2025;9(3):189–98.

[Downloaded from jommid.pasteur.ac.ir on 2026-11-16]

4. Liang W, Zhao Y, Meng Q, Jiang W, Deng S, Xue J. The role of long non-coding RNA in hepatocellular carcinoma. Aging (Albany NY). 2024;16(4):4052–73.
5. Zhang H, Liao Z, Liu F, Su C, Zhu H, Li Y, et al. Long noncoding RNA HULC promotes hepatocellular carcinoma progression. Aging (Albany NY). 2019;11(20):9111–27.
6. Xin X, Wu M, Meng Q, Wang C, Lu Y, Yang Y, et al. Long noncoding RNA HULC accelerates liver cancer by inhibiting *PTEN* via autophagy cooperation to miR15a. Mol Cancer. 2018;17(1):94.
7. Qiu L, Wang T, Xu X, Wu Y, Tang Q, Chen K. Long non-coding RNAs in hepatitis B virus-related hepatocellular carcinoma: regulation, functions, and underlying mechanisms. Int J Mol Sci. 2017;18(12):2505.
8. Elzein SM, Brombosz EW, Kodali S. Liver transplantation for cancer—current challenges and emerging solutions. J Clin Med. 2025;14(15):5365.
9. Yousef EH, El Gayar AM, El-Magd NFA. Insights into sorafenib resistance in hepatocellular carcinoma: mechanisms and therapeutic aspects. Crit Rev Oncol Hematol. 2025;212:104765.
10. Yoo SY, Badrinath N, Woo HY, Heo J. Oncolytic virus-based immunotherapies for hepatocellular carcinoma. Mediators Inflamm. 2017;2017:5198798.
11. Li Y, Shen Y, Zhao R, Samudio I, Jia W, Bai X, et al. Oncolytic virotherapy in hepato-bilio-pancreatic cancer: the key to breaking the log jam? Cancer Med. 2020;9(9):2943–59.
12. Moon H, Ro SW. MAPK/ERK signaling pathway in hepatocellular carcinoma. Cancers (Basel). 2021;13(12):3026.
13. Kazemi R, Ataei-Pirkooh A, Aghasadeghi MR, Modaresi MH, Hamidi-Fard M. Human reovirus serotype 3 effectively targets Huh-7 cells. Iran J Virol. 2020;14(2):23–8.
14. Kazemi R, Ataei-Pirkooh A, Aghasadeghi MR, Etemadzadeh MH, Alavian SM, Ghanaati H, et al. The effects of human reoviruses on cancer cells derived from hepatocellular carcinoma biopsies. Clin Lab. 2021;67(3):681–7.
15. Fu LY, Jia HL, Dong QZ, Wu JC, Zhao Y, Zhou HJ, et al. Suitable reference genes for real-time PCR in human HBV-related hepatocellular carcinoma with different clinical prognoses. BMC Cancer. 2009;9:49.
16. Gao Q, Wang XY, Fan J, Qiu SJ, Zhou J, Shi YH, et al. Selection of reference genes for real-time PCR in human hepatocellular carcinoma tissues. J Cancer Res Clin Oncol. 2008;134(9):979–86.
17. Tyler KL, Sokol RJ, Oberhaus SM, Le M, Karrer FM, Narkewicz MR, et al. Detection of reovirus RNA in hepatobiliary tissues from patients with extrahepatic biliary atresia and choledochal cysts. Hepatology. 1998;27(6):1475–82.
18. Radonić A, Thulke S, Mackay IM, Landt O, Siegert W, Nitsche A. Guideline to reference gene selection for quantitative real-time PCR. Biochem Biophys Res Commun. 2004;313(4):856–62.
19. Panzitt K, Tschernatsch MM, Guelly C, Moustafa T, Stradner M, Strohmaier HM, et al. Characterization of HULC, a novel gene with striking up-regulation in hepatocellular carcinoma, as noncoding RNA. Gastroenterology. 2007;132(1):330–42.
20. Rodríguez Stewart RM, Berry JT, Berger AK, Yoon SB, Hirsch AL, Guberman JA, et al. Enhanced killing of triple-negative breast cancer cells by reassortant reovirus and topoisomerase inhibitors. J Virol. 2019;93(23):e01411-19.
21. Müller L, Berkeley R, Barr T, Ilett E, Errington-Mais F. Past, present and future of oncolytic reovirus. Cancers (Basel). 2020;12(11):3219.
22. Berry JT, Muñoz LE, Stewart RMR, Selvaraj P, Mainou BA. Doxorubicin conjugation to reovirus improves oncolytic efficacy in triple-negative breast cancer. Mol Ther Oncolytics. 2020;18:556–72.
23. Jiffry J, Thavornwatanayong T, Rao D, Fogel EJ, Saytoo D, Nahata R, et al. Oncolytic reovirus (pelareorep) induces autophagy in *KRAS*-mutated colorectal cancer. Clin Cancer Res. 2021;27(3):865–76.
24. Pérez-Domínguez F, Quezada-Monrás C, Cárcamo L, Muñoz JP, Carrillo-Beltrán D. Oncolytic viruses as a novel therapeutic approach for colorectal cancer: mechanisms, current advances, and future directions. Cancers (Basel). 2025;17(11):1854.
25. Rastegarpanah M, Kafi ZZ, Negahdari B. *In vivo* tracking modalities for oncolytic reovirus: principles, clinical applications, and translational integration. Mol Imaging Biol. 2026;28(3):400–16.
26. Kitabayashi J, Shirasaki T, Shimakami T, Nishiyama T, Welsch C, Funaki M, et al. Upregulation of the long noncoding RNA HULC by hepatitis C virus and its regulation of viral replication. J Infect Dis. 2022;226(3):407–19.
27. Sharma G, Tripathi SK, Das S. lncRNA HULC facilitates efficient loading of HCV-core protein onto lipid droplets and subsequent virus-particle release. Cell Microbiol. 2019;21(10):e13086.
28. Liu Y, Feng J, Sun M, Yang G, Yuan H, Wang Y, et al. Long non-coding RNA HULC activates HBV by modulating HBx/STAT3/miR-539/APOBEC3B signaling in HBV-related hepatocellular carcinoma. Cancer Lett. 2019;454:158–70.
29. Meng XY, Luo Y, Anwar MN, Sun Y, Gao Y, Zhang H, et al. Long non-coding RNAs: emerging and versatile regulators in host–virus interactions. Front Immunol. 2017;8:1663.
30. Samson A, Bentham MJ, Scott K, Nuovo G, Bloy A, Appleton E, et al. Oncolytic reovirus as a combined antiviral and anti-tumour agent for the treatment of liver cancer. Gut. 2018;67(3):562–73.
31. Samudh N, Shrilall C, Arbuthnot P, Bloom K, Ely A. Diversity of dysregulated long non-coding RNAs in HBV-related hepatocellular carcinoma. Front Immunol. 2022;13:834650.
32. Sivasudhan E, Blake N, Lu Z, Meng J, Rong R. Hepatitis B viral protein HBx and the molecular mechanisms modulating the hallmarks of hepatocellular carcinoma: a comprehensive review. Cells. 2022;11(4):741.
33. Husein A, Jamal A, Kamal MA, Alqurashi YE, Al-Malki ES, Naiyer MM, et al. Hepatitis B virus-induced hepatocellular carcinoma: HBx-associated epigenetic mechanisms and therapeutic opportunities. Cancer Gene Ther. 2026;33:612–23.

[Downloaded from jommid.pasteur.ac.ir on 2026-11-16]

Cite this article:
Kazemi R, Hamidi-Fard M, Siasi E, Aghasadeghi MR, Rahimi P. Temporal Changes in Long Non-Coding RNA HULC Expression in Hepatitis B Virus-Associated Hepatocellular Carcinoma Cells Infected with Oncolytic Reovirus: An *In Vitro* Study. J Med Microbiol Infect Dis. 2026; 14 (3): 191-199.

[Downloaded from jommid.pasteur.ac.ir on 2026-11-16]